Applied Surface Science 335 (2015) 78–84

Contents lists available at ScienceDirect

Applied Surface Science

journal homepage: www.elsevier.com/locate/apsusc

Localized surface grafting reactions on carbon nanofibers induced by gamma and e-beam irradiation

M.C. Evora [a], J.R. Araujo [b,*], E.H.M. Ferreira [b], B.R. Strohmeier [c], L.G.A. Silva [d], C.A. Achete [b]

[a] Institute for Advanced Studies-IEAV/DCTA, Av. Cel Jose Alberto Albano do Amarante, 1-Putim, 12228-001 São Jose dos Campos, SP, Brazil
[b] Instituto Nacional de Metrologia, Qualidade e Tecnologia, Av. Nossa Sra. das Graças, 50, 25250-020 Duque de Caxias, RJ, Brazil
[c] Thermo Fisher Scientific, 5225 Verona Road, Madison, WI 53711, USA
[d] Institute for Nuclear and Energy Research- IPEN, Av. Prof lineu Prestes, 2242- Cidade Universitaria, 05508-000 SP, Brazil

ARTICLE INFO

Article history:
Received 15 October 2014
Received in revised form 1 February 2015
Accepted 3 February 2015
Available online 11 February 2015

Keywords:
Carbon nanofiber
X-ray photoelectron spectroscopy
Electron beam
Gamma-rays
Grafting reactions

ABSTRACT

Electron beam and gamma-ray irradiation have potential application to modify the carbon fiber nanostructures in order to produce useful defects in the graphitic structure and create reactive sites. In this study, the methodology to functionalize carbon nanofiber (CNF), via a radiation process and using acrylic acid as a source of oxygen functional groups, was investigated. The samples were submitted to a direct grafting radiation process with electron beam and gamma-ray source. Several parameters were changed such as: acrylic acid concentration, radiation dose and percentage of inhibitor necessary to achieve functionalization, with higher percentage of oxygen functional groups on CNF surface, and better dispersion. The better results achieved were when mixing CNF in a solution of acrylic acid with 6% of inhibitor ($FeSO_4 \cdot 7H_2O$) and irradiated at 100 kGy. The samples were characterized by X-ray photoelectron spectroscopy and the surface composition (atomic%) showed a significant increase of oxygen content for the samples after irradiation. Also, the dispersion of the functionalized CNF in water was stable during months which may be a good indication that the functionalization process of CNF via ionizing radiation was successful.

1. Introduction

Carbon nanofibers (CNFs) are being thoroughly investigated for application in structural composites for the aerospace industry. This requires careful control of their surfaces to promote properties required for end use because CNFs are not compatible with most polymers.

CNFs are cylindrical nanostructures composed of graphene layers that may take one of the several arrangements such as stacked cones. CNFs have also attracted attention in the last 10 years because they offer somewhat comparable electrical, mechanical, and thermal properties, at a lower production cost than SWCNTs and MWCNTs [1]. CNFs differ from SWCNTs and MWCNTs in the following respects: carbon nanofibers have an average diameter of 60–200 nm while carbon nanotubes have an average diameter of 10–20 nm, they are longer (30–100 μm) and they have a different surface morphology [2,3].

Advanced CNF–polymer nanocomposites can be obtained combining two specific properties: uniform dispersion of CNFs in the polymeric matrix and strong interfacial adhesion for efficient tension transfer from the polymeric matrix to the CNFs [4,5]. Likewise, CNFs without any surface treatment may have a weak interfacial adhesion with a polymeric matrix. Therefore, it is necessary to modify their surfaces through chemical or physical techniques to produce optimized polymer nanocomposites from a mechanical property view.

There are several methods to functionalize carbon-based materials and these modifications may promote changes in the (nanostructure) surface [6–12]. Some works investigate the impact of the process conditions on nanostructures and, consequently, on the technological applications of the final product. The main effects investigated are: composition of monomers and solvents employed in the functionalization [12–14], reaction temperature [12,15], additives [15], and dispersion of carbon materials in solvents and water [16–18].

Radiation process, with the aim to modify carbon-based materials, has been used for a long time and is a subject that still has plenty to be explored [19–26]. Ionizing radiation has high-enough energy to convert at least one neutral atom or a molecule into

* Corresponding author. Tel.: +55 21 21453045; fax: +55 21 26799021.
E-mail addresses: cecilia@ieav.cta.br (M.C. Evora), jraraujo@inmetro.gov.br (J.R. Araujo), lgasilva@ipen.br (L.G.A. Silva).

http://dx.doi.org/10.1016/j.apsusc.2015.02.024
0169-4332/

Table 1
Samples prepared with acrylic acid submitted to the direct radiation grafting process.

Sample name	Samples PR-25-PS-XT	Dose (kGy)		$FeSO_4 \cdot 7H_2O$ (%)
GA-1	Pristine	0	–	None
Blank-1	Pristine	0	–	1
Blank-2	Pristine	0	–	6
GA-11	Pristine	50	E-beam	6
GA-12	Pristine	100	E-beam	6
GA-13	Pristine	100	Gamma	6
GA-14	Pristine	100	Gamma	10
GA-16	Pristine	90	Gamma	6
GA-17	Pristine	90	E-beam	6
GA-18	E-beam pre-irradiated at 1000 kGy	90	E-beam	6

an ion pair. The energy employed by this radiation is localized in individual atoms or molecules, and it is sufficiently high to break and induce chemical reactions in a short period of time. This is the basic principle of using ionizing radiation to chemically modify materials. Therefore, radiation grafting polymerization may be an alternative way to induce surface modification, and it is a uniform, effective, and environment-friendly method. It can be conducted at room temperature and in gas, liquid, and solid-state phases. To date, there are some published papers related to radiation grafting polymerization to functionalize graphitic nanostructures [2,9,11] but this subject still draws some attention because several structural transformations may occur in carbon nanostructures under the irradiation process. Characterization, control, and reproducibility are still a challenge when particle size is in the nanometer range and it is not an easy task to compare methods of characterization which are usually not in agreement with each other.

The aim of this work was to investigate and to propose a methodology for functionalization of CNFs and compare two different methods to promote grafting reactions: gamma-ray and electron beam irradiation. Different parameters, such as inhibitor concentration in acrylic acid solution, were applied to the samples during the process to establish this methodology. X-ray photoelectron spectroscopy (XPS) was used to evaluate the functionalization degree and the rearrangement of the Csp^2 hybridization of the CNFs after irradiation processes, comparing the two methods tested. Raman spectroscopy was used to investigate the nanostructure of carbon samples after irradiation and is a usual nondestructive tool for structural characterization of carbon materials.

2. Material and methods

2.1. Sample preparation

CNFs used in this study were obtained from Applied Sciences Inc. Cedarville Ohio (under licenses from General Motors Corp. and Applied Science Inc.) and they are manufactured in a continuous vapor phase growth process that contributes to a significantly lower cost compared to most carbon nanotubes, and they are readily available in large quantities and in several grades.

CNFs (PR-25-PS grade) were selected for the investigation in this work because, in a previous work, they showed to be less resistant under an electron beam process and it was possible to promote surface oxidation [26]. CNF has a chemically vapor deposited (CVD) layer of carbon on the surface of a graphitic tubular core fiber. CNFs are available in different grades. The PS grade is produced at 1100 °C by pyrolytically cleaning of the as-produced CNF, and to remove polyaromatic hydrocarbons from the surface.

Table 1 enrolls the samples submitted to the direct radiation grafting process. As-received PR-25-PS-XT samples were weighted, and then immersed in solutions of 10% of acrylic acid (MERK/stabilized with 200 ppm of hydroquinone) with 1, 6 or 10% of inhibitor metal salt ($FeSO_4 \cdot 7H_2O$). One part of the sample was poured into Petri dishes and irradiated with a direct accelerator operated by the Instituto de Pesquisas Energéticas e Nucleares (IPEN- São Paulo/Brazil). These samples were irradiated with an industrial electron accelerator Dynamitron, from Radiation Dynamics Inc., model DC 1500/25-JOB 188 operating with the following parameters: beam energy 1.5 MeV, pulse current 5.62 mA, 5 kGy/pass with a dose rate of 22.42 kGy/s. The other part of the sample, with the same amount of acrylic acid and $FeSO_4 \cdot 7H_2O$, was irradiated by the gamma radiation process in a Cobalt-60 irradiator, Gammacell model 220, series 142, manufactured by Atomic Energy of Canada Limited whose activity is 64.946 TBq (1755.1 Ci)—06/2012. The Gammacell design provides uniform gamma field and the samples were irradiated at a dose rate of 1.48 kGy/h. The mixtures were purged with dry nitrogen for 10 min to remove dissolved oxygen and then sealed.

2.2. Characterization

The surface oxygen content of the nanofibers was characterized by X-ray Photoelectron Spectroscopy (XPS) analysis. The XPS analyses of GA-1, Blank-1, GA-12, GA-13, and GA-14 samples were conducted in a K-Alpha XPS equipment from Thermo Fisher Scientific, with a 400 μm X-ray spot size and with the low energy electron gun for charge neutralization system turned on. XPS survey spectra (0–1350 eV) were collected for all samples to provide qualitative and quantitative surface analysis information. XPS measurements of GA-1, Blank-2, GA-16, GA-17, and GA-18 samples were carried out at National Institute of Metrology, Quality and Technology (Inmetro). X-ray photoelectron spectroscopy (ESCAplus P System; Omicron Nanotechnology; Taunusstein, Germany) was used in order to study the chemical composition and chemical groups in carbon nanofibers before and after an irradiation process. The XPS analyses were performed using an Al Kα=1486.7 eV X-ray source, 10^{-10} mbar base pressure and 10^{-8} mbar during the analysis, with a 20 mA emission at a voltage of 13.5 kV. Survey spectra were acquired in the range of 1350–0 eV, step of–0.8 eV, dwell time of 0.2 s, and analyzer pass energy of 70 eV. For carbon, the high-resolution spectra were obtained with analyzer pass energy of 30 eV. No charging effects were observed (C 1s binding energy peak ~284.4 eV). The peak fitting was performed using the CasaXPS software. Before the peak fitting, the background was subtracted using a Shirley function. This software introduces the classical parameters (intensity, binding energy, line-width, Gaussian/Lorentzian mixing ratio) for symmetrical lines and the exponential tail parameters for asymmetrical ones. X-ray-excited Auger electron spectroscopy (X-AES) C KLL peaks were acquired in the kinetic range of 180–300 eV and using a step of −0.1 eV.

Raman analyses were carried out in a Renishaw InVia Reflex spectrometer equipped with a peltier cooled CCD and using an 1800 gr/mm grating. The samples were deposited onto a glass slide, and the spectra were collected using a 20x (NA 0.40) objective in a backscattering configuration. The excitation energy was 2.41 eV from the 514.5 nm line of an argon laser. Spot size was approximately 2 μm and low power (below 100 μW) was used in order to avoid sample graphitization. For each sample, a set of 10 spectra were collected at different points in the interval of 1050 to 1950 cm^{-1}. All the spectra were treated to subtract the background and the peaks were fitted using Lorentzian curves.

3. Results and discussion

Fig. 1 shows the results of the dispersion of the samples Blank-2, GA-16, GA-17, and GA-18. The samples were dispersed in water

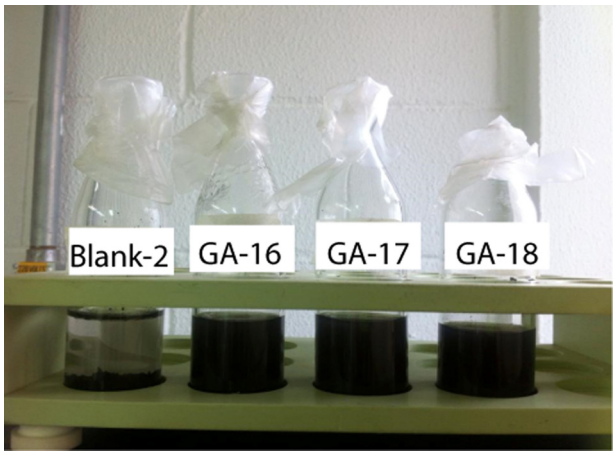

Fig. 1. Illustration of Blank-2, GA-16, GA-17, and GA-18 dispersed after 70 days.

under the sonication process for 1 h. This picture was taken 70 days after the dispersion process. The functionalized samples via radiation grafting presented good dispersion after 70 days.

XPS survey spectra (0–1350 eV) were collected for all samples to provide qualitative and semi-quantitative surface analysis information (Fig. 2). The O/C atomic ratios calculated from XPS survey spectra are an important feature in order to compare non-irradiated and irradiated samples. The increase of the O/C atomic ratio is an indication of the effectiveness of the grafting process. The surface composition (atomic%) showed a significant increase of oxygen content for the samples irradiated (Table 2), and for this reason, they offer excellent and very stable dispersion. The O surface concentration varied from 5.1 up to 20.3 at% among the tested samples. The O 1s spectra were similar for all samples showing a single, broad, asymmetric peak centered at 533.0–533.1 eV, which is typical for oxygen-containing functional groups on carbon surfaces such as C–O, C=O, and O=C–OH.

Survey XPS spectra of carbon nanofibers as received (GA-1), irradiated with 90 kGy of gamma-rays (GA-16) or with the same dose of e-beam (GA-17), and pre-irradiated at 1000 kGy before e-beam irradiation, are compared in Fig. 2. Some traces of contaminant elements, as S and Fe, are observed in the XPS spectrum of all analyzed samples, which can be attributed to traces of the inhibitor metal salt, $FeSO_4$, together with the other contaminant elements. The N surface concentration varied from 0.6 up to 1.6 at% among the samples. N 1s spectra were similar for all seven samples showing broad, multiple peaks and/or shoulders in the binding energy range of ~398–403 eV, which indicates the presence of most likely three organic nitrogen-containing species. Low intensity Si peaks were observed (0.2–0.5 at%). Their origin may be due to the silicon tape used to fix the carbon nanofibers on the sample holder or contaminant. Si 2p binding energies observed (i.e., ~102.3–102.9 eV) were characteristic of organic silicon species (e.g., silicones and/or silicates) for all samples. Silicon dioxide (~103.3–103.7 eV) was not detected.

Fig. 3 shows the effect of the irradiation method on the functionalization of the carbon nanofibers. Non irradiated sample (GA-1) showed mainly C=C bonds and a shake-up satellite peak ($\pi \rightarrow \pi^*$, 291.4 eV) characteristic of aromatic C structures [27–30]. This transition is attributed to the delocalized π conjugation, characteristic of an aromatic C structure. This process appears in the photoemission spectrum, such as a secondary peak (satellite shake-up), in the side of the primary peak (C sp^2) with lower kinetic energy due to the energy loss by excitation. A binding energy of 284.1 eV essentially corresponds to non-functionalized sp^2 carbons which would be expected for CNF materials. The sample irradiated with 100 kGy of gamma radiation (GA-13) showed more intensity in the peak characteristic of HO–C=O group (~ 289.3 eV) than the sample irradiated with the same dose of e-beam (GA-12) which is an indication that the grafting process was more effective using gamma radiation. These two radiation sources promotes different primary events of interactions with the matter (knock on and electromagnetic interaction), but the major interaction is still Compton scattering for both sources with generation of secondary electrons. The secondary electron is responsible for initiating the ionization events that produce free radicals. Even the major interaction is similar, it is important to point out that the absence of mass and charge gives gamma a far greater penetration and it delivers lower dose rates which may lead to different results. Electron beam delivers much higher dose rate leading to heating and contributing to generate various rearrangements of the carbon atoms [31].

Among several parameters that influence the grafting reaction, absorbed dose is a very important one. Absorbed dose is the energy absorbed per unit mass which promotes excitation and ionization event as a consequence of the electronic interactions of the incident electrons with orbital electrons. The free radical generated by the ionization process is proportional to the absorbed dose [19]. The effect of the irradiation doses on the graphitization level of the carbon nanofibers is showed in Fig. 3 b and c. In Fig. 3b, the samples irradiated with e-beam showed an increase in the intensity of the carboxyl peak with the increase of the irradiation dose (from 50 to 100 kGy). This amount of energy was sufficient to increase the carboxyl functionality in the e-beam irradiated sample. However, a lower e-beam dose increase, 10 kGy, was not observed as significant improvement in the functionalization. Dose increase of 10 kGy of gamma-ray on CNFs shows similar results, Fig. 3c.

Fig. 4 shows C1s XPS spectra and the peak components obtained through mathematical fitting (see Methods for details) of carbon nanofibers, pristine (Fig. 4a) and irradiated with 90 kGy of gamma-rays (Fig. 4b), 90 kGy of e-beam (Fig. 4c) and the sample pre-irradiated with 1000 kGy before irradiation with 90 kGy of e-beam (Fig. 4d).

Carbon nanofibers were fitted using six different components. The CNF components were assigned as the typical core-level photoelectron line of carbonaceous materials [27–30]. The component C1 (284.4 ± 0.2 eV) is attributed to undamaged alternant hydrocarbon structure while the component C2 (285.4 ± 0.2 eV) is attributed to damaged alternant hydrocarbon structure. The component C3 (286.3 ± 0.2 eV) is less resolved and has been assigned as sp^3 free radical defects or C–O bonds (the proximity of the binding energies of these two chemical sites overlaps their signals). The same has been reported with the component C4 (287.1 ± 0.3 eV) which is attributed to C=O (carbonyl groups) or to the $\pi \rightarrow \pi^*$ shake-up satellite peak of the C2 component. The component C5 (289.3 ± 0.3 eV) is attributed to O–C=OH groups (carboxyl) and C6 (291.1 ± 0.1 eV) is attributed to the $\pi \rightarrow \pi^*$ shake-up satellite peak of the component C1.

The C 1s spectra obtained for the irradiated samples indicated the presence of various amounts of C–O–C, C=O, and O=C–OH surface functional groups. The samples GA-16 (gamma irradiation) and GA-17 (e-beam irradiation) had the highest intensity peaks for the O=C–OH group (~289.2 eV). The intensity of $\pi \rightarrow \pi^*$ shake-up peaks (~291.1 eV) decreased after irradiation: in pristine sample its component contributed with 5.1% of the envelope fitted while in the samples irradiated, this percentage was ~ 2.0. This band is assigned to graphitic carbon band [28,30], thus, the radiation changes the carbon nanofiber surface from a graphitic structure to an oxidized carbon-functionalized structure. The reduction of shake-up satellite peak is attributed to the reduction of electrons in conjugated and aromatic structure. Corroborating this evidence, undamaged alternant hydrocarbon structure (Csp^2) component

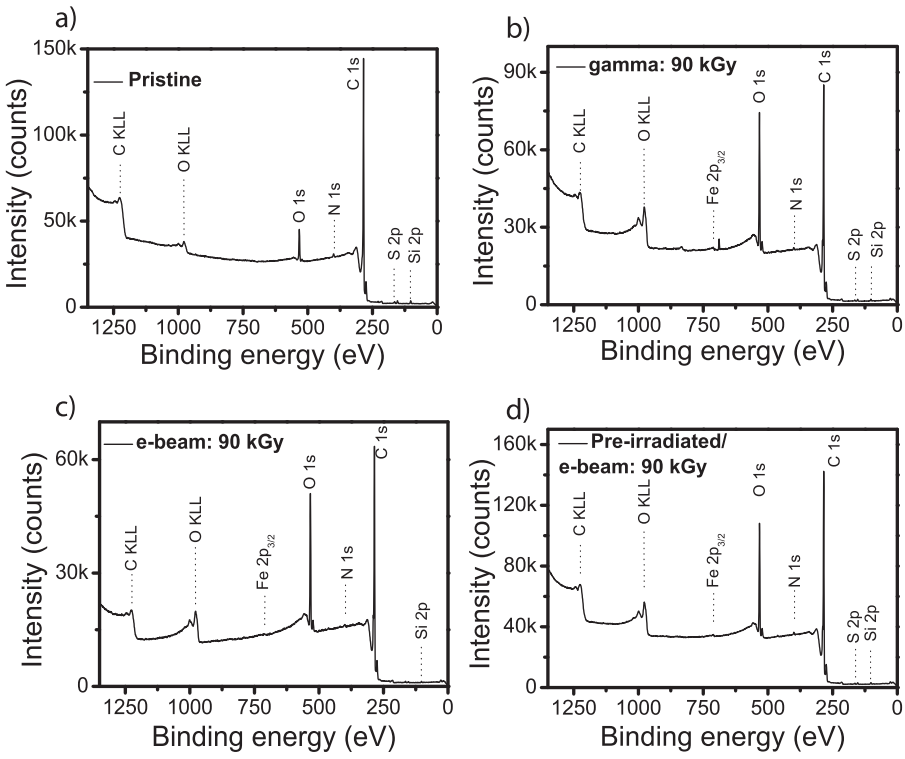

Fig. 2. XPS survey spectra of PR-25-PS sample non-irradiated (GA-1), irradiated with 90 kGy of gamma-rays (GA-17), irradiated with 90 kGy of e-beam and the sample pre-irradiated with 1000 kGy and after irradiated with 90 kGy of e-beam (GA-18).

Table 2
Surface compositions (atomic%) and O/C atomic ratios calculated from XPS survey spectra (see Methods) for carbon nanofibers as received (GA-1), non-irradiated samples (Blank-1 and Blank-2) and irradiated samples (GA-11, GA-12, GA-13, GA-14, GA-16, GA-17, and GA-18.

at (%)	GA-1	Blank 1[a]	Blank 2	GA 11[a]	GA 12[a]	GA 13[a]	GA 14[a]	GA 16	GA 17	GA 18
C	93.1	90.6	90.2	83.1	79.7	78.4	81.5	80.6	81.6	82.9
O	5.1	7.0	7.6	14.6	18.4	20.3	16.8	18.4	17.1	15.8
N	1.1	1.6	1.4	1.4	0.9	0.9	0.9	0.6	0.9	0.9
Fe	0.1	0.1	0.2	0.1	0.1	0.1	0.2	0.1	0.1	0.1
S	0.5	0.4	0.5	0.4	0.3	0.2	0.4	0.2	0.2	0.2
Na, Cl	0.1	0.3	0.1	0.4	0.6	0.1	0.2	0.1	0.1	0.1
O/C	0.05	0.08	0.08	0.18	0.23	0.26	0.21	0.23	0.21	0.19

[a] Analyzed in K-Alpha XPS equipment from Thermo Fisher Scientific.

was also reduced after irradiation (Table 3) because defects, such as dangling bonds, vacancies, interstitial, pentagon–heptagon pair defects, may be created in the graphene structure during irradiation.

The X-ray induced CKLL Auger spectra were similar for the six samples but did show some minor differences in peak shape and position. It has been shown [32–34] that, after differentiation, C KLL Auger spectra can give important information

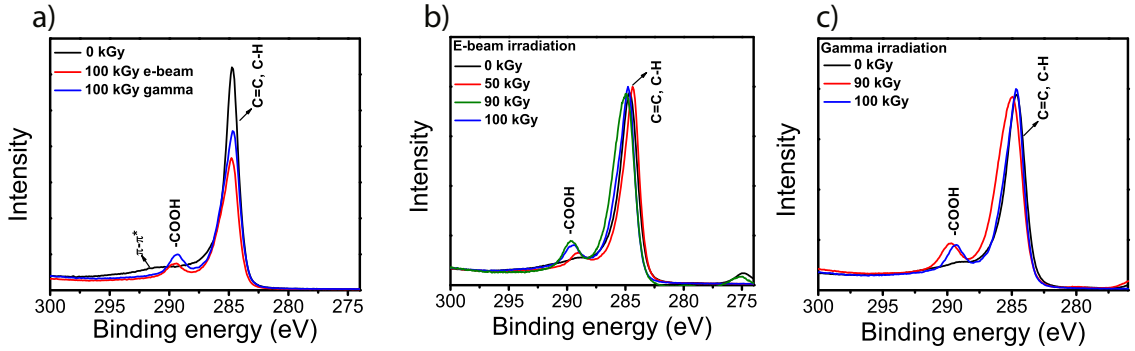

Fig. 3. C1s XPS spectra comparing: (a) PR-25-PS pristine non-irradiated (GA-1), irradiated with 100 kGy of e-beam (GA-12), and irradiated with 100 kGy of gamma radiation (GA-13); (b) PR-25-PS with 6% of inhibitor ($FeSO_4{\cdot}7H_2O$) irradiated with different doses of e-beam radiation (0, 50, 90, and 100 kGy); these samples correspond to Blank-2, GA-11, GA-12, and GA-17 in Table 1; (c) PR-25-PS with 6% of inhibitor ($FeSO_4{\cdot}7H_2O$) irradiated with different doses of gamma radiation (0, 90, and 100 kGy); these samples correspond to Blank-2, GA-16, and GA-13 in Table 2.

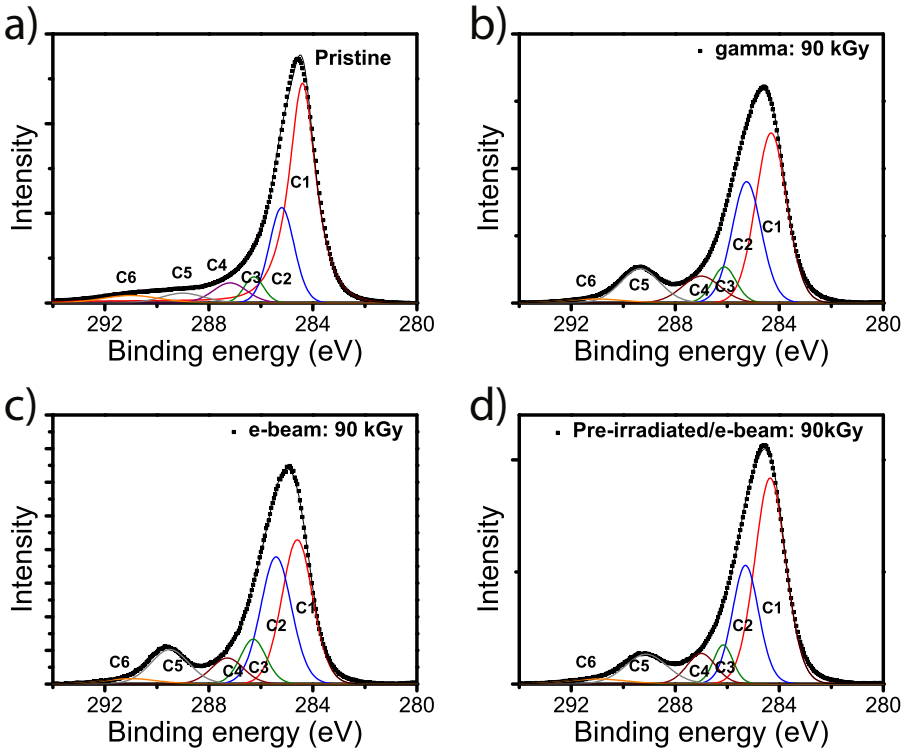

Fig. 4. (a) XPS C 1s spectra of PR-25-PS sample non-irradiated (GA-1), (b) irradiated with 90 kGy of gamma-rays (GA-17), (c) irradiated with 90 kGy of e-beam, and (d) the sample pre-irradiated with 1000 kGy before irradiation with 90 kGy of e-beam (GA-18). The C1–C6 components were fitted using Gauss/Lorentz function. The C 1s peaks are assigned as: C1, undamaged alternant hydrocarbon structure (C=C) at 284.4 eV; C2, damaged alternant hydrocarbon structure (C=C) at 285.3 eV; C3, unresolved carbon–oxygen single bund (C–O) and sp^3 free radical (CH_3) at 286.1 eV; C4, unresolved carbonyl groups (C=O) or $\pi \rightarrow \pi^*$ shake-up satellite peak of the C2 component at 287.1 eV; C5, carboxyl groups (COOH) at 289.3 eV; and C6, $\pi \rightarrow \pi^*$ shake-up satellite peak of the component C1 at 291.1 eV.

Table 3
Binding energies (eV), full-width at half maximum (FWHM), and the percentage of each C 1s component.

Chemical group/sample	Binding energy (eV)				FWHM				(%)			
	GA-1	GA-16	GA-17	GA-18	GA-1	GA-16	GA-17	GA-18	GA-1	GA-16	GA-17	GA-18
C1	284.4	284.3	284.6	284.4	1.4	1.4	1.4	1.4	58.9	42.7	37.1	50.1
C2	285.2	285.3	285.4	285.3	1.1	1.3	1.4	1.2	14.5	29.0	32.8	24.7
C3	286.0	286.1	286.3	286.2	1.2	1.1	1.2	0.9	8.6	6.9	9.7	6.0
C4	287.1	287.0	287.3	287.0	1.7	1.7	1.5	1.3	8.2	8.4	7.0	6.9
C5	289.0	289.3	289.5	289.1	1.9	1.8	1.7	1.9	4.7	11.0	11.0	9.9
C6	291.2	291.1	291.0	291.0	2.7	2.7	2.4	2.7	5.1	2.0	2.4	2.4

regarding the relative amount of sp^2 and sp^3 bonding in carbon materials by the so-called Auger "D-parameter". The C KLL data were differentiated to give the Auger "D-parameter," which is the energy separation between the primary "hill" and "valley" of the differentiated spectrum (Fig. 5a). The measured Auger D-parameter for sample GA-1 was 21.6 (Fig. 5b), a similar value to the literature reference for graphite [32]. This result indicates a significant amount of undamaged sp^2 bonding on the surface of the non-irradiated sample, which is consistent with the $\pi \rightarrow \pi^*$ shake-up satellite peak observed in the XPS

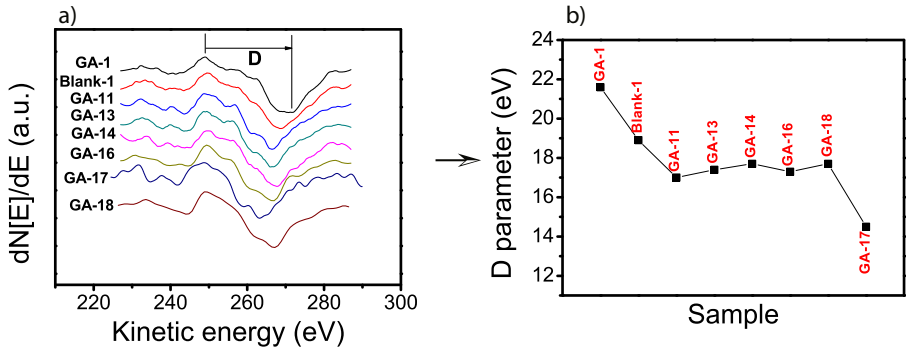

Fig. 5. (a) Differentiated X-ray-induced Auger C KLL peaks of carbon nanofiber samples pristine (GA-1, Blank-1) and irradiated samples (GA-11, GA-13, GA-14, GA-16, GA-17, and GA-18); (b) Auger D-parameter evaluated measuring the separation between the primary "hill" and "valley" of the differentiated spectrum.

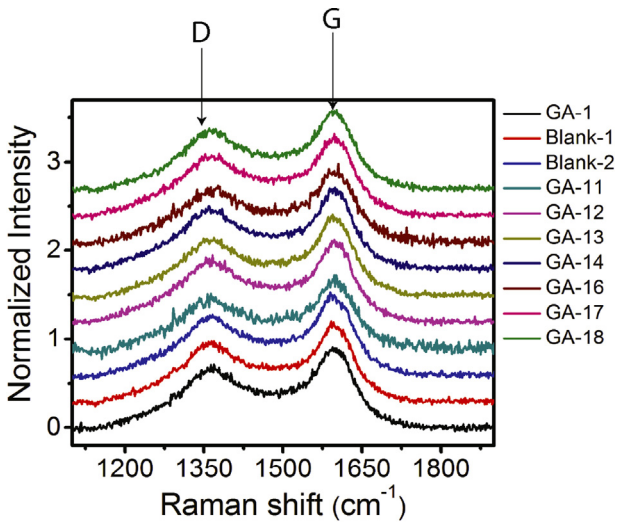

Fig. 6. Raman spectroscopy results of PR-25-PS irradiated at 1000 kGy, soaked into monomers solution with water/methanol (50% vol) and washed with deionized water to remove the residual monomers and by products.

C1s peak results, and is expected for carbon nanofiber materials.

The Auger D-parameter for the samples irradiated (GA-11, GA-12, GA-13, GA-14, GA-16, and GA-18, Fig. 5b) ranged between 17.0 and 17.7 indicating that these samples had less sp^2 and, probably, more defects in their graphitic structure compared to samples GA-1 and Blank-1. This is an indication of C=C bond breaking, and subsequently the formation of new damage sp^2 or sp^3 carbon atoms bonded with oxygen functional groups on the CNT surface. The sample GA-17 showed the lower D-parameter among the tested samples (14.5), which corroborates with XPS results in which GA-17 also showed the highest C2 component percentage (a damaged hydrocarbon structure contributes with 32.8% of the envelop fitted), Table 3.

The samples were characterized by Raman spectroscopy and the results are shown in Fig. 6. Generally, the Raman spectra of carbon materials are simple, with two most intense bands between 1000 and 2000 cm^{-1}. The peaks near 1580 and 1350 cm^{-1} correspond to the C=C in-plane stretching mode (called the G band) and the disorder induced (D band), respectively. The intensity ratio of the D band to the G band (ID/IG) in the Raman spectra has been widely used to evaluate the disorder in sp^2 hybridized carbon systems [35].

Fig. 6 shows one representative Raman spectrum for each sample. All samples have the same characteristic spectrum of a defective carbon material, showing wide D and G bands with similar intensities. Table 4 summarizes the results of fitting all spectra with two Lorenztian peaks and taking the mean ID/IG ratio for each sample. Those ratios are very similar, implying that there are no meaningful changes in the carbon nanofiber bulk structure. The same results have been found and published before. High radiation dose was unable to damage the bulk of the PR-25-PS structure. It was localized on the surface and did not compromise the core of the carbon nanofiber. [25].

Table 4
Intensity ratio of the D band to the G band (ID/IG) for all samples.

Sample	ID/IG	Uncertainty ($k=2$)
GA-1	0.748	0.026
Blank-1	0.761	0.031
Blank-2	0.740	0.025
GA-11	0.737	0.058
GA-12	0.771	0.030
GA-13	0.708	0.027
GA-14	0.757	0.027
GA-16	0.746	0.055
GA-17	0.776	0.039
GA-18	0.759	0.024

At first, this result would not to be expected, since gamma rays have, in general, a deep penetration in the material. E-beam has, typically, a shorter penetration than the gamma rays, but, as Pregler et al. [36] have shown in their research on carbon nanotubes, this is not surface limited either. In our work, however, further considerations must be done.

First, this process was carried out in acrylic acid solution. Acrylic acid monomers contain an unsaturated C=C double bond which degrades easily under the radiation process. Second, the energy of gamma rays and the electron beam is absorbed by all elements of the system, in which the water usually absorbs most of this energy [37]. In addition, depending on the amount of energy involved in the process (considering primary and secondary electrons from the cascade effect), defects (dangling bonds, vacancies, interstitial, pentagon–heptagon pair defects) are created in the graphene structure, and a high strain at the sites of defects should be considered [38]. With defects expanding, the increased tensile force leads to a less stable structure compared with perfect hexagonal carbon network. The vacancies along the carbon nanostructure tend to recombine with the interstitial carbon atom displaced during the radiation process [39]. CNFs have a very organized core and are covered by a thin layer of turbostratic carbon. This turbostratic layer is the lesser organized external layer of CNF, less resistant to radiation, and is the layer that will receive the primary knock on to start the displacement of the atom process.

Thus, the advantage of this process is that the overall graphitic structure has not been damaged. The radiation grafting reaction occurs mainly in the outer layer, which is less organized than the bulk of the wall. Raman spectroscopy is a bulk characterization technique in which the laser penetration greatly exceeds the thickness of the turbostratic carbon layer deposited on the nanofiber surface where the oxidation takes place. In general, the graphite structure of the nanofiber core did not show any damage.

4. Conclusions

Radiation-induced graft copolymerization is a method to modify materials with many advantages. The goal of the present study was to investigate the use of ionizing radiation to functionalize carbon nanofibers with several monomers. The experiments were set up in order to determine the optimum radiation dose and inhibitor content required for this process to take place using the existing irradiators.

The samples which were added to a solution of acrylic acid with 6% of inhibitor, and after irradiated with electron beam and gamma source at 100 kGy dose, presented higher oxygen content and better dispersion. The increase of the O/C atomic ratio is an indication of the effectiveness of the grafting process. The surface composition (atomic%) showed a significant increase of oxygen content for the samples irradiated, which varied from 5.1 up to 20.3 at% among the tested samples. The O 1s spectra were similar for all samples showing a single, broad, asymmetric peak centered at 533.0–533.1 eV, which is typical for oxygen-containing functional groups on carbon surfaces such as O–C, C=O, and O=C–OH. The Auger D-parameter for the samples irradiated ranged between 14.5–17.7 indicating that these samples had less undamaged Csp^2 and more defects compared to non-irradiated samples. The intensity of the $\pi \rightarrow \pi^*$ shake-up peak (~291.5 eV) decreased after irradiation and it was attributed to the reduction of electrons in the graphitic structure on the CNF surface. An important remark concerning Raman results is that the radiation-induced graft copolymerization process did not

damage the overall graphitic structure of carbon nanofibers. Thus, using the irradiation methods tested in this study, the radiation grafting reaction mainly occurred in the outer layer.

Acknowledgements

We acknowledge Fapesp project 2011/12510-8 and International Atomic Energy Agency project RC: 16647 (F2-RC-12071) for the financial support. We also would like to thank Elizabeth Somessari and Carlos Gaia da Silveira from Institute Nuclear Energy and Research for the radiation support and Applied Science Inc for providing the carbon nanofibers.

References

[1] A. Eitan, K. Jiang, D. Dukes, R. Andrews, L.S. Schadler, Surface modification of multiwalled carbon nanotubes: toward the tailoring of the interface in polymer composites, Chem. Mater. 15 (2003) 3198–3201.
[2] K. Lafdi, W. Fox, M. Matzek, E. Yildiz, Effect of carbon nanofiber heat treatment on physical properties of polymeric nanocomposites—part I, J. Nanomater. 2007 (2007) 52729.
[3] K. Lafdi, W. Fox, M. Matzek, E. Yildiz, Effect of carbon nanofiber-matrix adhesion on polymeric nanocomposite propertiespart II, J. Nanomater. (2008) 310126.
[4] H. Yu, X. Mo, J. Peng, M. Zhai, J. Li, G. Wei, X. Zhang, J. Qiao, Radiation-induced grafting of multi-walled carbon nanotubes in glycidyl methacrylate–maleic acid binary aqueous solution, Radiat. Phys. Chem. 77 (2008) 656–662.
[5] L.G. Pedroni, J.R. Araujo, M.I. Felisberti, A.F. Nogueira, Nanocomposites based on MWCNT and styrene–butadiene–styrene block copolymers: effect of the preparation method on dispersion and polymer–filler interactions, Compos. Sci. Technol. 72 (2012) 1487–1492.
[6] D. Long, G. Wu, G. Zhu, Noncovalently modified carbon nanotubes with carboxymethylated chitosan: a controllable donor-acceptor nanohybrid, Int. J. Mol. Sci. 9 (2008) 120–130.
[7] X. Zhang, T.V. Sreekumar, T. Liu, S. Kumar, Properties and structure of nitric acid oxidized single wall carbon nanotube films, J. Phys. Chem. B 108 (2004) 16435–16440.
[8] S.R. Wang, Z.Y. Liang, T. Liu, B. Wang, C. Zhang, Effective amino-functionalization of carbon nanotubes for reinforcing epoxy polymer composites, Nanotechnology 17 (2006) 1551–1557.
[9] J.I. Paredes, A. Martínez-Alonso, J.M.D. Tascón, Oxygen plasma modification of submicron vapor grown carbon fibers as studied by scanning tunneling microscopy, Carbon 40 (2002) 1101–1108.
[10] Y.-R. Shin, I.-Y. Jeon, J.-B. Baek, Stability of multi-walled carbon nanotubes in commonly used acidic media, Carbon 50 (2012) 1465–1476.
[11] V. Brüser, M. Heintze, W. Brandl, G. Marginean, H. Bubert, Surface modification of carbon nanofibres in low temperature plasmas, Diamond Relat. Mater. 13 (2004) 1177–1181.
[12] G. Wei, K. Shirai, K. Fujiki, H. Saitoh, T. Yamauchi, N. Tsubokawa, Grafting of vinyl polymers onto VGCF surface and the electric properties of the polymer-grafted VGCF, Carbon 42 (2004) 1923–1929.
[13] S.H. Choi, Y.C. Nho, Radiation-induced graft copolymerization of mixture of acrylic acid and acrylonitrile onto polypropylene film, Korea Polym. J. 6 (1998) 287–294.
[14] C.V. Chaudhari, Y.K. Bhardwaj, S. Sabharwal, Radiation grafting of methyl methacrylate on radiation crosslinked natural rubber film, J. Radioanal. Nucl. Chem. 267 (2005) 113–119.
[15] J.H. Chen, G. Wei, Y. Maekawa, M. Yoshida, N. Tsubokawa, Grafting of poly(ethylene-block-ethylene oxide) onto a vapor grown carbon fiber surface by gamma-ray radiation grafting, Polymer 44 (2003) 3201–3207.
[16] S.M. Chen, G.Z. Wu, Y.D. Liu, D.W. Long, Preparation of poly(acrylic acid) grafted multiwalled carbon nanotubes by a two-step irradiation technique, Macromolecules 39 (2006) 330–334.
[17] C.-H. Jung, D.-K. Kim, J.-H. Choi, Surface modification of multi-walled carbon nanotubes by radiation-induced graft polymerization, Curr. Appl. Phys. 9 (2009) S85–S87.
[18] A.L. Martinez-Hernandez, C. Velasco-Santos, V.M. Castano, Carbon nanotubes composites: processing, grafting and mechanical and thermal properties, Curr. Nanosci. 6 (2010) 12–39.
[19] M.C. Clochard, J. Bègue, A. Lafon, D. Caldemaison, C. Bittencourt, J.J. Pireaux, N. Betz, Tailoring bulk and surface grafting of poly(acrylic acid) in electron-irradiated PVDF, Polymer 45 (2004) 8683–8694.
[20] J. Chen, Y. Maekawa, M. Yoshida, N. Tsubokawa, Radiation grafting of polyethylene onto conductive carbon black and application as a novel gas sensor, Polym. J. 34 (2002) 30–35.
[21] X. Chen, K. Yoon, C. Burger, I. Sics, D. Fang, B.S. Hsiao, B. Chu, In-situ X-ray scattering studies of a unique toughening mechanism in surface-modified carbon nanofiber/UHMWPE nanocomposite films, Macromolecules 38 (2005) 3883–3893.
[22] X. Ping, M. Wang, G. Xuewu, Surface modification of poly(ethylene terephthalate) (PET) film by gamma-ray induced grafting of poly(acrylic acid) and its application in antibacterial hybrid film, Radiat. Phys. Chem. 80 (2011) 567–572.
[23] M. Sammalkorpi, A.V. Krasheninnikov, A. Kuronen, K. Nordlund, K. Kaski, Irradiation-induced stiffening of carbon nanotube bundles, Nucl. Instrum. Methods Phys. Res. B: Beam Int. Mater. Atoms 228 (2005) 142–145.
[24] N. Tsubokawa, Functionalization of carbon material by surface grafting of polymers, Bull. Chem. Soc. Jpn. 75 (2002) 2115–2136.
[25] M.C. Evora, D. Klosterman, K. Lafdi, L. Li, J.L. Abot, Functionalization of carbon nanofibers through electron beam irradiation, Carbon 48 (2010) 2037–2046.
[26] C.H. Jung, J.S. Lee, D.K. Kim, I.T. Hwang, Y.C. Nho, J.H. Choi, Surface functionalization of single-walled carbon nanotubes by a radiation grafting, Appl. Chem. 13 (2009) 25–28.
[27] J. Filik, P.W. May, S.R.J. Pearce, R.K. Wild, K.R. Hallam, X.P.S. laser, Raman analysis of hydrogenated amorphous carbon films, Diamond Relat. Mater. 12 (2003) 974–978.
[28] R. Rozada, J.I. Paredes, S. Villar-Rodil, A. Martinez-Alonso, J.M.D. Tascon, Towards full repair of defects in reduced graphene oxide films by two-step graphitization, Nano Res. 6 (2013) 216–233.
[29] J. Díaz, G. Paolicelli, S. Ferrer, F. Comin, Separation of the sp^3 and sp^2 components in the C1s photoemission spectra of amorphous carbon films, Phys. Rev. B 54 (1996) 8064–8069.
[30] A. Ganguly, S. Sharma, P. Papakonstantinou, J. Hamilton, Probing the thermal deoxygenation of graphene oxide using high-resolution *in situ* X-ray-based spectroscopies, J. Phys. Chem. C 115 (2011) 17009–17019.
[31] L. Woo, C.L. Sandford, Comparison of electron beam irradiation with gamma processing for medical packaging materials, Radiat. Phys. Chem. 63 (2002) 845–850.
[32] S. Turgeon, R.W. Paynter, On the determination of carbon sp2/sp3 ratios in polystyrene–polyethylene copolymers by photoelectron spectroscopy, Thin Solid Films 394 (2001) 43–47.
[33] S. Kaciulis, Spectroscopy of carbon: from diamond to nitride films, Surf. Interface Anal. 44 (2012) 1155–1161.
[34] J.C. Lascovich, R. Giorgi, S. Scaglione, Evaluation of the sp^2/sp^3 ratio in amorphous-carbon structure by XPS and XAES, Appl. Surf. Sci. 47 (1991) 17–21.
[35] M.S. Dresselhaus, A. Jorio, A.G. Souza Filho, R. Saito, Defect characterization in graphene and carbon nanotubes using Raman spectroscopy, Philos. Trans. R. Soc. A: Math. Phys. Eng. Sci. 368 (2010) 5355–5377.
[36] S.K. Pregler, S.B. Sinnott, Molecular dynamics simulations of electron and ion beam irradiation of multiwalled carbon nanotubes: the effect on failure by inner tube sliding, Phys. Rev. B 73 (2006) 224106.
[37] Y.H.F. Al- qudah, G.A. Mahmoud, M.A.A. Khalek, Radiation crosslinked poly(vinyl alcohol)/acrylic achi copolymer for removal of heavy metal ions from aqueous solutions, J. Radiat. Res. Appl. Sci. 7 (2014) 135–145.
[38] O.V. Yazyev, I. Tavernelli, U. Rothlisberger, L. Helm, Early stages of radiation damage in graphite and carbon nanostructures: A first-principles molecular dynamics study, Phys. Rev. B 75 (2007) 115418.
[39] U. Ritter, P. Scharff, C. Siegmund, Radiation damage to multi-walled carbon nanotubes and their Raman vibrational modes, Carbon 44 (2006) 2694–2700.